CRACK PROPAGATION AND DAMAGE IN METALLIC ALLOYS

E. Bouchaud [1] and F. Paun [2]

[1]DSM/DRECAM/SPCSI, CEA-Saclay
91191 Gif-Sur-Yvette Cedex, France
[2]DMMP, ONERA
B.P. 72, 29 Av. du Général Leclerc,
92322 Châtillon Cedex

ABSTRACT

The morphology of damage cavities in an aluminium alloy is investigated with an Atomic Force Microscope (AFM) and shown to be the same as the one exhibited at small length scales by fracture surfaces. These observations support a scenario of crack propagation which takes explicitely damage into account.

KEYWORDS

Scaling, Roughness, Quantitative fractography, Atomic Force Microscopy, Damage.

INTRODUCTION

The renewed interest for the morphology of fracture surfaces and crack fronts [1-4] has given rise to a considerable theoretical effort [5-12]. However, no model to this day is entirely satisfactory. Among the various questions one can ask about the basic hypothesis of these models, the question of damage appears to be crucial. The central point of the present paper is to show that damage has to be explicitely taken into account to be able to predict the observed scaling properties.

As a matter of fact, fracture surfaces of various materials have been shown to be self-affine, sometimes on more than five decades of length scales [2-4,13]. They actually exhibit two self-affine regimes, observed both on metallic alloys and on glass, with exponents $\zeta_c \simeq 0.5$ at small length scales, and $\zeta \simeq 0.8$ at larger length scales [2-4,13,14]. The crossover length ξ_c separating the two regimes has been observed to decrease with the average crack front velocity [2,4]. Although models of lines propagating through randomly distributed microstructural heterogeneities are in principle able to predict such a behaviour, the most refined of them [9] fails to reproduce the experimental observations.

The basic hypothesis of these models which is questioned here is relative to damage: can one define a crack front at all scales of observation within the scaling domain ? The answer is yes as long as the scale of observation is smaller than the size of independent damage cavities. It does not make any sense at larger length scales.

The scenario we have in mind both for the ductile fracture of metals and plausibly, at very different length scales, for the fracture of amorphous materials [15-17], is the following: cavities nucleated on the sites of the material heterogeneities extend giving rise to a roughness exponent close to 0.5 as long as they are isolated. The 0.8 roughness exponent is the result of the coalescence of these cavities (small cavities merge together and also join the main crack), which are likely to be intercorrelated.

To test this idea, actually inspired by the results obtained from Molecular Dynamics simulations on amorphous ceramics [15-17, we have investigated the morphology of damage cavities appearing during fracture in an aluminium alloy.

Material and experimental techniques

The material is an Al-Cr-Zr alloy, constituted by flakes of rapidly quenched ribbons consolidated by extrusion. The microstructure is shown [18,19] to be quite anisotropic, for the flakes align in the direction of extrusion, which happens to be also the direction of crack propagation in this case. The alloy is made of elongated strips of material parallel to this direction, with alternately coarse intermetallic precipitates (diameter 0.5-1 μm)and much finer ones (diameter 0.1μm). In the strips containing fine precipitates, the grains of the α matrix are elongated in the direction of extrusion, and flattened along the plane of the plate. Their thickness is of order 1μm, and their length can reach several tens of micrometers. In the strips containing coarse precipitates, the grains are rather equiaxed, and the smallest ones are of the order of 1μm. Two types of intermetallic phases are identified, one is $Al_{13}Cr_2$ with precipitates sizes in the range 40-300 nm, and the other one, Al_3Zr (metastable), appears in the form of extremely fine precipitates about 10nm in size. No porosity is detected in the material prior to fracture, although, because of the poor consolidation (the extrusion temperature remains moderate in order to avoid a coarsening of the fine hardening precipitates as well as a return to thermodynamic equilibrium of the metastable phases), it cannot be excluded.

Chevron notched bar specimens are submitted to mode I tension. The geometry of the specimen is such that the crack actually progresses between the flakes. Crack propagation is stopped before complete failure. The sample is cut and polished as shown in Fig. 1 to allow for two sets of observations (at different depths of cut) of the damaged zone ahead of the crack tip. The distance between the two planes of cut is 0.5mm, larger than all the microstructural lengths.

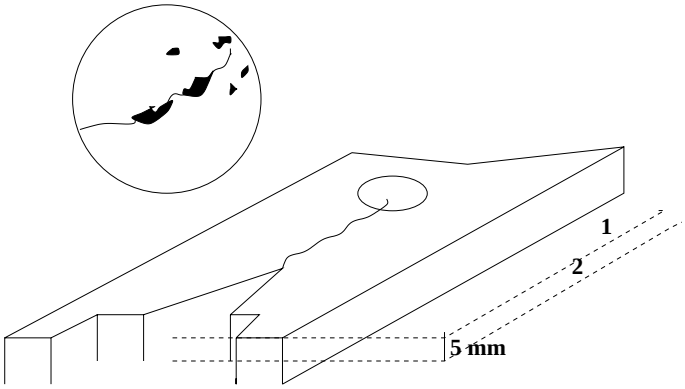

Figure 1: Sample preparation for the observation of the damaged zone ahead of the main crack tip. The two cuts (planes 1 and 2) are distant by 0.5 mm. The damaged zone ahead of the crack tip is explored in Atomic Force Microscopy.

Experimental results

The observations are performed with an Atomic Force Microscope (AFM). An AFM image of the crack tip zone is shown in Fig. 2.

In what follows we distinguish “large” and “small” cavities. The large cavities are quite anisotropic in shape (see Fig. 2, these cavities are elongated in the direction of the main crack), with dimensions 10-100μm. Furthermore, they are visibly linked to the main crack. Small cavities are much more isotropic in shape, and their dimensions are close to 3-5μm. They seem to be independent of the main crack.

Large and small cavities have a very different structure at a fine scale, as shown in Fig. 3. We will see later that this qualitative difference actually reflects a quantitative difference in roughness.

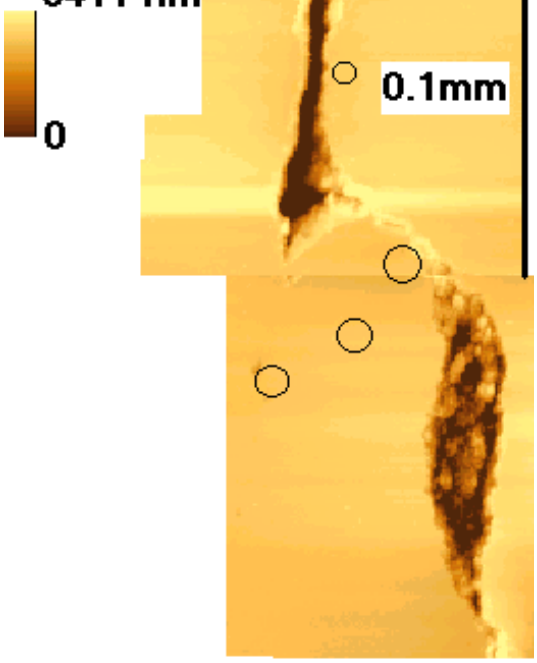

Figure 2: AFM image of the crack tip. One can observe a large cavity visibly related to the main crack. The circles indicate the location of small cavities which seem independant of the main crack.

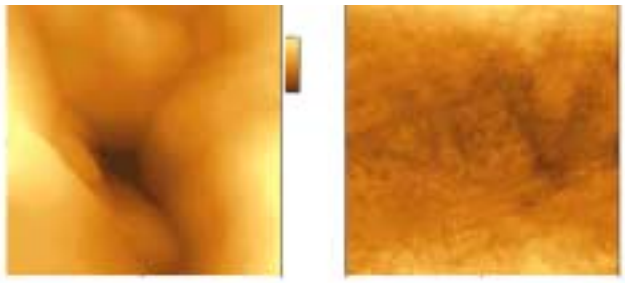

Figure 3: AFM image of a large (left, image size) and a small cavity (right 1.02μmx1.02μm, image size 2.5μmx2.5μm) at a comparable magnification, showing the difference in structure.

In each explored cavity 10 profiles containing 1000 points (corresponding to distances ranging from 1.13 to 10 micrometers) are registered in two directions (parallel and perpendicular to the direction of crack propagation). In each case, these profiles are analysed with two different methods - namely the Hurst method and the power spectrum method [20] - in order to determine the roughness exponent. For each cavity, an average of both the min-max difference $\Delta Z_{max}(r)$ and the power spectrum $P(q)$ is performed, with consistent results.

In both cases, contrary to what can be observed for their shape, large cavities appear to be isotropic, while small ones present an anisotropy between the parallel and perpendicular directions.

As an example, an average of the power spectrums of 10 parallel profiles and 10 perpendicular profiles are shown in Fig. 4 for one large cavity. The best fit is a power law with exponent 2.53, corresponding to a roughness index ζ equal to 0.77. This is consistent with the result of the Hurst analysis, for which a roughness exponent 0.79 is measured.

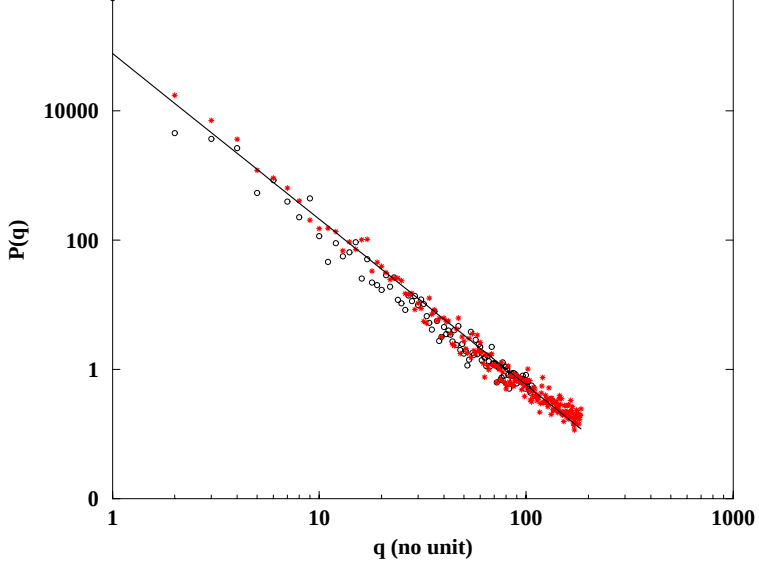

Figure 4: Average over the power spectra of 10 parallel (o) and 10 perpendicular ($\star$) profiles. The best fit is a power law with exponent -2.53 in both cases (solid line).

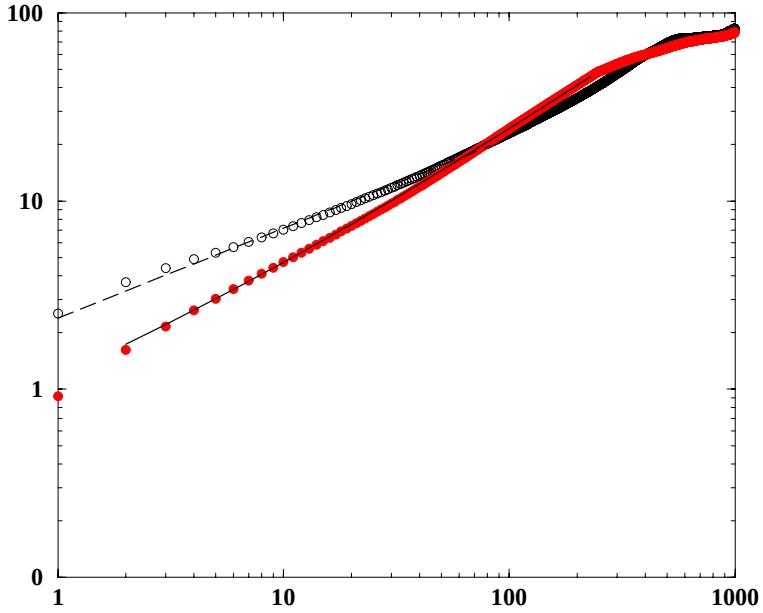

Figure 5: Average over the power spectra of 10 parallel ($\bullet$) and 10 perpendicular (o) profiles. The best fits correspond to one power law with exponent 0.48 (dashed line) in the case of perpendicular profiles and to a function corresponding to two asymptotic regimes (0.5 at small length scales, 0.78 at larger ones, with a crossover at 6 nm) in the case of parallel profiles (solid line).

The structure of small cavities is more complex, since they do not only exhibit the two regimes self-affine regimes (0.5 and 0.8), but are also anisotropic. Fig. 5 shows the evolution of $\Delta Z_{max}(r)$ for 10 parallel and 10 perpendicular profiles in the case of a small cavity in the AlCrZr alloy. For profiles parallel to the direction of crack propagation, one can see the two asymptotic regimes (roughness exponents 0.5 and 0.8), while along the perpendicular direction, only the 0.5 regime is present. This behaviour is reproduced in all the small cavities we observe, for the two planes of cut.

We have shown that “large” cavities, linked to the main crack are isotropic and reveal only, in the present case, the roughness index 0.8. On the contrary, “small” independent cavities have a more complex structure: they only exhibit the 0.5 regime in a direction perpendicular to crack propagation, and the two regimes in the direction of the main crack.

This supports the following scenario [21] for crack propagation: when cavities grow by themselves, their acquire a roughness characterized by a 0.5 exponent. The 0.8 exponent exhibitted at larger length scales is directly linked to the coalescence of such cavities.

The fact that the 0.8 exponent is also observed at larger length scales in small cavities may be the sign that these damage defects are the result of the coalescence of smaller cavities. This is true only in the direction of crack propagation, where coalescence is as a matter of fact more likely to occur. Note that this is not the case for the Molecular Dynamics simulations results however [15-17], where only the 0.5 exponent is observed. It might be due to the smaller sample sizes, and to the higher crack speeds (coalescence has no time to occur before the cavity joins the main crack).

At length scales smaller than a cavity size before coalescence, a crack front can perfectly be defined. In principle, line models [8-11] might be able to predict the 0.5 roughness in this case. However, an other hypothesis has been made elsewhere [22], suggesting that crack front waves [23-25] might be responsible for the roughening at these small length scales. This model leads as a matter of fact to a 1/2 roughness index independently of the microstructure, and to material-dependent length scales.

At larger length scales, one cannot define a crack front, because of the very existence of the assembly of damage cavities. These cavities, growing in mutual interaction under the action of a high stress triaxiality due to the presence of the main crack, are probably strongly correlated “geometrically”: the presence of a given cavity will favour or prevent the opening of an other one in a certain domain, and probably influence its growth rate. Our conjecture is that these correlations are at the origin of the non-trivial 0.8 exponent observed on various types of materials (see [2] and references therein). One has now to address the question of universality of this exponent, when damage correlations of different natures must be considered. The similarity of the crack growth mode and the differences in the scales at which this phenomenon occurs might however be a clue to understand universality in exponents and differences in relevant length scales [2].

It has been shown in the case of fracture surfaces that the crossover length decreases with the average crack velocity. In the new scenario imagined here, this crossover length is the size of cavities at coalescence, and cavities have more time to grow before coalescence if the average crack velocity is smaller.

One can also wonder why only the 0.8 exponent is seen in large cavities. This may be due to the intensity of the local stress field: cavities joining the main crack are very likely in zones of higher stresses than cavities which are not crossed by the crack. These cavities coalesce more rapidly than cavities located in regions of lower stresses, and hence, having less time to grow before coalescence takes place, reach a size ξ_c at coalescence which is significantly smaller, and might be unreachable at our scales of observation.

Finally, it has been shown elsewhere [13] that the self-affine correlation length, i.e. the upper bound of the scaling domain, is of the order of the grain size for metallic materials. Damage correlations are likely to disappear when there is a change in the crystalline orientation, and hence, we believe that this self-affine correlation length might as well be viewed as a damage correlation length.

One limitation of our study, however, concerns the direction of the observed profiles in cavities as compared to the direction of profiles observed on fracture surfaces. Cavities can be explored either in a direction parallel to crack growth or perpendicular to it, but they can only be studied within a plane containing the tensile direction (see Fig. 1). On the contrary, fracture profiles on post mortem specimens are both perpendicular to the direction of crack propagation and to the tensile axis. In other words, the roughness exponents measured on fracture surfaces are inaccessible as far as cavities are concerned.

However, the clear differences in morphology exhibitted by the independent cavities and the ones linked to the main crack strongly support the idea of two relevant processes, one being linked to the growth of isolated damage defects, and the other one to their coalescence.

1. B.B. Mandelbrot, D.E. Passoja, A.J. Paullay, Nature **308** 721 (1984).
2. E. Bouchaud, J. Phys./ Condens. Matter **9**, 4319 (1997).
3. P. Daguier, S. Hénaux, E. Bouchaud and F. Creuzet, Phys.Rev. E **53**, 5637 (1996).
4. P. Daguier, B. Nghiem, E. Bouchaud, F. Creuzet, Phys. Rev. Lett. **78**, 1062 (1997).
5. J. Schmittbuhl, S. Roux, J.-P. Vilotte, K. J. Maloy, Phys. Rev. Lett. **74**, 1787 (1995).
6. G. G. Batrouni, A. Hansen, Phys. Rev. Lett. **80**, 325 (1998).
7. V. I. Räisänen, E. T. Seppala, M. J. Alava, P. M. Duxburry, Phys. Rev. Lett. **80**, 329 (1998).
8. J.-P. Bouchaud, E. Bouchaud, G. Lapasset, J. Planès, Phys. Rev. Lett., **71**, 2240, (1993) ; E. Bouchaud, J.-P. Bouchaud, J. Planès, G. Lapasset, Fractals, **1**, 1051, (1993).
9. S. Ramanathan, D. Ertaş, D. S. Fisher, Phys. Rev. Lett. **79**, 873 (1997).
10. S. Ramanathan, D. S. Fisher, Phys. Rev. Lett. **79**, 877 (1997).
11. S. Ramanathan, D. S. Fisher, Phys. Rev. B **58**, 6026 (1998).
12. D. Ertaş, M. Kardar, Phys. Rev. Lett. **69**, 929 (1992); D. Ertaş, M. Kardar, Phys. Rev. E **48**, 1228 (1993).
13. E. Bouchaud,P. Daguier, M. Hinojosa, B. Nghiem, Bulletin Mecamat (1998).
14. E. Bouchaud, S. Navéos, J. Physique I **5**, 547 (1995).
15. A. Nakano, R. K. Kalia, P. Vashishta, Phys. Rev. Lett. **73** , 2336 (1994).
16. A. Nakano, R. K. Kalia, P. Vashishta, Phys. Rev. Lett. **75** , 3138 (1995).
17. P. Vashishta, R. Kalia, A. Nakano, Computing in Science and Engineering, p. 56, september/october (1999).
18. E. Bouchaud, L. Kubin, H. Octor, Metall. Trans. A, **22A**, 1021 (1991).
19. E. Bouchaud, H. Octor, T. Khan, Materials and Design **14**, 29 (1993).
20. J. Schmittbuhl, J.P. Vilotte, S. Roux, Phys. Rev. E **51**, 131 (1995).
21. E. Bouchaud, F. Paun, Computing in Science and Engineering, p. 32, september/october (1999).
22. E. Bouchaud, J.-P. Bouchaud, D. S. Fisher, S. Ramanathan, J. R. Rice, in preparation.
23. J. W. Morrissey, J. R. Rice, EOS Trans. Amer. Geophys. Un. **77**, F485 (1996).
24. J. W. Morrissey, J. R. Rice, J. Mech. Phys. Solids **46**, 467 (1998).
25. J. W. Morrissey, J. R. Rice, J. Mech. Phys. Solids **48**, 1229 (2000).
26. E. Bouchaud, G. Lapasset, J. Planès, Europhys. Lett. **13**, 73 (1990).
27. K. J. Maloy, A. Hansen, E.L. Hinrichsen, S. Roux, Phys. Rev. Lett. **68**, 213 (1992).